Multi-parameter Bifurcation Analysis of the South-Brazilian Power System

A. A. P. Lerm, *Member, IEEE*, C. A. Cañizares, *Senior Member, IEEE*, and A. S. e Silva

***Abstract*—This paper presents a detailed bifurcation analysis of real multi-parameter power systems. Equilibrium points are used to evaluate the system eigenvalues, obtain different bifurcation diagrams and evaluate the stability for two systems, i.e. a simple theoretical system to illustrate the basic concepts and highlight the main issues, and the southern section of the Brazilian network to demonstrate how these ideas can be applied to a real power system. The paper studies the influence of soft and hard-limits and AVR droop on the systems, using detailed generator models. The stability regions and the effect that various parameters and bifurcations have on them are studied in detail.**

***Index Terms*—Small-perturbation stability, voltage stability, bifurcation analysis, stability regions, generator control limits.**

I. Introduction

Various types of stability problems in power systems, such as voltage collapse and oscillatory phenomena, can be analyzed through bifurcation theory [1]. Thus, bifurcation analysis has become an important analysis tool in stability studies of power networks. This paper extends the work presented in [2] to a practical and detailed study of a real test system, to show the influence of various system parameters, control limits and settings in the bifurcation analysis and stability of an actual power system. Although the general theory on which the paper is based is well known [3], and has been thoroughly studied in power systems [1], there are no references in the literature to applications of this theory to actual power systems; furthermore, most of the published work concentrates on single-parameter bifurcation studies. Hence, this paper addresses these shortcomings by applying bifurcation theory to study the effect of multi-parameter variations on the stability of a real power network, using complex load and generator models that include detailed voltage regulator representations.

Typically, the bifurcations associated with different stability problems are local bifurcations, and hence they can be studied through eigenvalues of the linearization around operating points of the differential-algebraic equations (DAE) used to model the system. These equilibria are typically obtained from load flow analysis, due to the simplicity of its formulation, obtaining a variety of operating points as certain system parameters change (usually the load). These points are then used to create the well-known nose or PV curves, identifying stable operating regions based on the results of the eigenvalue analysis. Although in some particular cases, nose curves may actually represent bifurcation diagrams [4], in most practical cases that is not the case [5]. Thus, the authors in [5] and [6] show that there are other implicit independent parameters that must be taken into account to qualify the stability regions on the PV curves obtained from a conventional power flow analysis. For example, a generator is assumed to have a constant terminal voltage in the power flow model; however, if the corresponding AVR is modeled in detail, the voltage set-point for this controller should change at each point on the PV curve to account for voltage droop, and thus keep the terminal voltage constant. To study these kinds of problems, a multi-parameter bifurcation analysis is required, which is the main topic of discussion in this paper.

A fairly comprehensive summary of the various types of bifurcations that can be encountered in power systems models is presented in [7], where the authors present a complete taxonomy of the different stability regions of large dynamical systems, considering that the parameter space is composed by *typal regions* (regions of structural stability) bounded by bifurcation surfaces. These surfaces are determined by different kinds of bifurcations, such as saddle-node, Hopf, singularity-induced and limit-induced bifurcations. Limit-induced bifurcations are somewhat particular to power systems and are due to controller limits in the system [8], [9], particularly generator reactive power limits; in many practical cases, these bifurcations are the main cause for voltage collapse problems, rather than saddle-node bifurcations. Two simple test systems modeled in detail are used in [10] to study their stability as one parameter (the load) changes, defining stability regions associated with all these bifurcations in the PV curves. In the current paper, all these bifurcations are considered to study the stability regions of a real power system as various parameters change in the system.

Finally, the authors in [11] use transient energy functions to study the effect of saddle-node bifurcations on the stability regions of power system equilibria, showing that as the system approaches the saddle-node, the stability region decreases until it becomes "zero" at the bifurcation, i.e. the perturbations that the system can withstand decrease as the system approaches the bifurcation point. The author in [12] uses also energy functions to show how shunt and series

Accepted for publication *IEEE Trans. Power Systems*, Oct. 2002.

A. A. P. Lerm is with the E & ARQ School, Catholic University of Pelotas, Pelotas, RS, 96010-000, Brazil, alerm@atlas.ucpel.tche.br

C. A. Canizares is with the Department of Electrical and Computer Engineering at the University of Waterloo, 200 University Av. W., Waterloo, ON, Canada, N2L-3G1, c.canizares@ece.uwaterloo.ca

A. S. e Silva is with the Dept. of Electrical Engineering, Fed. Univ. of Santa Catarina, 88040-900, Florianópolis, SC, Brazil, aguinald@labspot.ufsc.br

This work was partially supported by the Brazilian Government agency CAPES and NSERC, Canada.

reactive power compensation affect these stability regions. The energy function technique cannot be used to study the effect on the stability regions of bifurcations where equilibrium points do not merge (e.g., Hopfs); hence, the current paper illustrates the effect of these bifurcations on stability using actual time domain simulations for a given perturbation, so that relative sizes of the actual system stability regions can be determined.

This paper is organized as follows: Section 2 briefly discusses some of the theoretical foundations of bifurcation analysis of power systems, using as an example a 3-bus system to show the typical behavior of different bifurcation manifolds when controller droops and limits are considered. Section 3 presents the complete bifurcation analysis of the 213-bus South-Brazilian system, demonstrating the effect of several load models, generator controls and their limits on the corresponding bifurcation diagrams and system stability regions. Finally, Section 4 summarizes the main contributions of this paper, discussing as well possible future research directions.

II. Bifurcation Analysis

Nonlinear dynamical systems, such as those obtained from certain power system models, can be generically described by ordinary differential equations (ODE), i.e.

$$\dot{x} = f(x, \lambda, p) \tag{1}$$

where $x \in \Re^n$ corresponds to the state variables; $\lambda \in \Re^l$ represents a particular set of "non-controllable" scalar parameters that drive the system to a bifurcation in a quasi-static manner, i.e. as λ changes, the system steadily moves from equilibrium point to equilibrium point; $p \in \Re^k$ represents a series of "controllable" parameters associated with control settings; and $f: \Re^n \times \Re^l \times \Re^k \rightarrow \Re^n$ is a nonlinear vector field.

Typical power system models used in stability analysis present an additional difficulty, as these systems are modeled with a set of differential and algebraic equations (DAE) of the form

$$\begin{bmatrix} \dot{x} \\ 0 \end{bmatrix} = \begin{bmatrix} f(x, y, \lambda, p) \\ g(x, y, \lambda, p) \end{bmatrix} = F(z, \lambda, p) \tag{2}$$

where $x \in \Re^n$ typically stands for state variables corresponding to various system devices, such as generators, and their controls, that are defined by the nonlinear vector field $f: \Re^n \times \Re^m \times \Re^l \times \Re^k \rightarrow \Re^n$; the vector $y \in \Re^m$ represents the set of algebraic variables associated with the nonlinear algebraic function $g: \Re^n \times \Re^m \times \Re^l \times \Re^k \rightarrow \Re^m$, which typically correspond to load bus voltages and angles, depending on the load models used; $\lambda \in \Re^l$ stands for slow varying parameters that are typically associated with changing loading levels, over which operators have no direct control; and $p \in \Re^k$ represents the control settings that operators directly or indirectly control, such as AVR reference set-points or shunt compensation. Finally, $F = (f,g)$ and $z = (x,y)$.

The stability of DAE systems is thoroughly discussed in [13], demonstrating that if $D_y g(x,y,\lambda,p)$ can be guaranteed to be nonsingular along system trajectories, the behavior of (2) is primarily determined by the local ODE reduction

$$\dot{x} = f(x, y^{-1}(x, \lambda, p), \lambda, p) \tag{3}$$

where $y = y^{-1}(x,\lambda,p)$ results from the application of the Implicit Function Theorem to the algebraic constraints $g(x,y,\lambda,p)=0$ on the trajectories of interest. Equilibrium points of (2), i.e. points where $F(z_o,\lambda_o,p_o) = 0$, which have a singular $D_y g|_o$ are known as singularity-induced bifurcation points and are characterized by an eigenvalue of the state matrix

$$A = D_x f|_o - D_y f|_o \left[D_y g|_o\right]^{-1} D_x g|_o \tag{4}$$

changing from $+\infty$ to $-\infty$, or vice versa [7], [14].

A. Equilibria and Steady-state Operating Points

In power system stability analysis, equilibria are actually defined using a subset of equations typically referred to as the power flow equations,

$$G(z'_o, \lambda_o, p'_o) = G|_o = 0 \tag{5}$$

where z' and p' are subsets of z and p, respectively, and $G(z'_o,\lambda_o,p'_o) \subset F(z_o,\lambda_o,p_o)$. Thus, the typical procedure is to first solve the power flow equations (5) and then, based on the corresponding solutions, find equilibrium points of the dynamic model before proceeding with stability analysis of the full set of dynamic equations (2). For some particular system models, power flow solutions may correspond to actual system equilibria and vice versa [4], [15]. However, for most realistic dynamic and power flow models, the solution of the power flow equations does not guarantee the existence of an actual system equilibrium, as solutions of $G|_o = 0$ do not necessarily guarantee that $F|_o = 0$, and vice versa; this is particularly important for the discussions presented below regarding bifurcation diagrams.

Even when the proper system equilibria are available, i.e. the equilibrium points are directly computed from system equations (2), some p parameters must change in order to model standard steady-state operating procedure. In other words, some of the parameters p must be interchanged with some of the z variables, to then solve $F|_o = 0$ to obtain the desired operating points. For example, AVR set points are determined from (optimal) power flow analyses to obtain a desired voltage profile in the network.

B. Local Bifurcations

Standard bifurcation theory deals with the study of the stability of ODE system (1) which moves from equilibrium to equilibrium as the parameters λ change slowly [3], [16]; these bifurcation concepts can be directly extended to DAE systems (2) [4], [17].

There are several types of bifurcations associated with the changes of λ, some are local and some are global, depending on the behavior of the system dynamic manifolds and equilibrium points. The current paper concentrates only on the analysis of local bifurcations, which can be detected and analyzed by monitoring the eigenvalues of the state matrix (4). The following is a list of the generic, local bifurcations that are most likely to be encountered in power systems:

- *Node Focus (NF)*: These types of bifurcations are characterized by a complex conjugate pair of eigenvalues merging into one real eigenvalue, or vice versa, as the parameters λ change slowly. Although there is no real consequence for the system in practice, since no significant change on the stability of the system occurs, these bifurcations seem to be the precursors of other types of bifurcations [10], in particular for Hopf bifurcations, as discussed in [18].
- *Saddle-node (SN)*: These bifurcations, also known as turning points or fold bifurcations, are typically identified by a couple of equilibrium points merging at the bifurcation point and then locally disappearing as the slow varying parameters λ change. Many cases of actual voltage collapse in power systems have been associated with saddle-node bifurcations. This bifurcation corresponds to an equilibrium point (z_o,λ_o,p_o) where the state matrix (4) has a unique zero eigenvalue, and certain transversality conditions are met, distinguishing it from other types of "singular" bifurcations (transcritical and pitchfork) [3], [16], [19].
- *Hopf (HP)*: These bifurcations are characterized by a complex conjugate pair of eigenvalues crossing the imaginary axes of the complex plane from left to right, or vice versa, as the λ parameters slowly change. These types of bifurcations have been associated with a variety of oscillatory phenomena in power systems [1], and are typical precursors of chaotic motions [3], [16].
- *Limit-induced (LI)*: These bifurcations correspond to equilibrium points where system control limits are reached as the parameters λ slowly change, with the corresponding eigenvalues undergoing instantaneous changes that may affect the stability status of the system [7], [8]. Of particular interest are those bifurcation points where two equilibria merge and vanish, similarly to a SN bifurcation but without the state matrix (4) becoming singular.
- *Singularity-induced (SI)*: These bifurcations, as previously explained, are due to a singularity of the algebraic equations' Jacobian $D_y g|_o$, and correspond to equilibrium points where an eigenvalue of the state matrix (4) changes from +/-∞ to -/+∞. This sudden change of value is quite different from what is observed in the LI case, as the eigenvalues of the state matrix go from a large positive to a large negative number or vice versa, whereas for the LI these changes are "small".

All bifurcations were detected by monitoring the eigenvalues of the state matrix (4) as the system "moved" from one equilibrium point to another with changes in the system parameters.

C. Example

In this section, the previous theory is used to study load changes in the hypothetical 3-bus test system shown in Fig. 1. One of the generators is assumed to be an infinite bus, whereas the other generator is modeled using 5 differential equations (2 for the mechanical dynamics, 3 for the transient dynamics), plus a simple AVR with droop (transfer function $K_{AVR}/(1+T_{AVR}S)$), and no governor. Changes in the active power demand are picked up by the infinite bus. The data for this system is shown in Table I.

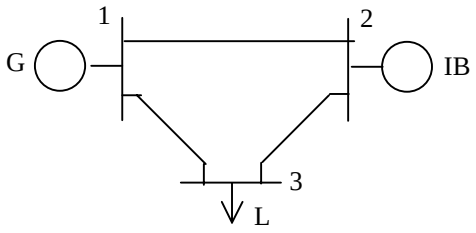

Fig. 1. Three-bus sample system.

TABLE I
P.U. DATA FOR 3-BUS SAMPLE SYSTEM.

H	10.0 s	τ'_{do}	8.5 s	P_{lo}	0.8
X_d	0.9	τ''_{do}	0.03 s	Q_{lo}	0.6
X_q	0.8	τ''_{qo}	0.9 s	V_{t2}	1.0
X'_d	0.12	P_m	1.0	$X_{1\text{-}2}$	0.2
X''_d	0.08	K_{AVR}	50.0	$X_{2\text{-}3}$	0.2
X''_q	0.08	T_{AVR}	0.5 s	$X_{1\text{-}3}$	0.2

In spite of the small size of this system, the qualitative results obtained for it can be readily extended to large real power systems, as shown in the next section. All simulations are carried out modeling the load as static constant power, with the bifurcation parameter λ representing the active and reactive power load changes at bus 3 as follows:

$$\begin{aligned} P_l &= P_{lo}(1+\lambda) \\ Q_l &= Q_{lo}(1+\lambda) \end{aligned} \tag{6}$$

where P_{lo} and Q_{lo} are the initial values shown in Table I. In this case, the AVR reference set-point V_{ref} corresponds to the controllable parameter p.

To analyze the influence of limits on the bifurcation diagrams, results are first obtained for the case with no limits on E_{fd}, and then compared to the case where limits are considered. In both cases, V_{ref} is varied within a relatively wide range of values to study its effect on the system bifurcations.

1) Case without limits: The results obtained in this case are shown in Figs. 2 and 3, where the voltage V_3 at Bus-3 is plotted as function of V_{ref} and λ. Figure 3 is just a projection and zoom-in of Fig. 2. For each value of V_{ref} one can observe that the system has 4 basic bifurcations. Thus, the system first becomes unstable through an HP bifurcation, which is then followed by NF, SI and SN bifurcations, in that order. The HP bifurcation occurs when a complex conjugate pair of stable eigenvalues crosses over the imaginary axis, from left to right. At the NF bifurcation, the complex pair of unstable eigenvalues changes to two real eigenvalues in the right-hand side of the complex plane (unstable NF). One of the positive real eigenvalues then moves to the left-hand side through a SI bifurcation from -∞ to +∞, while the other eigenvalue becomes zero at the SN bifurcation, which corresponds to the

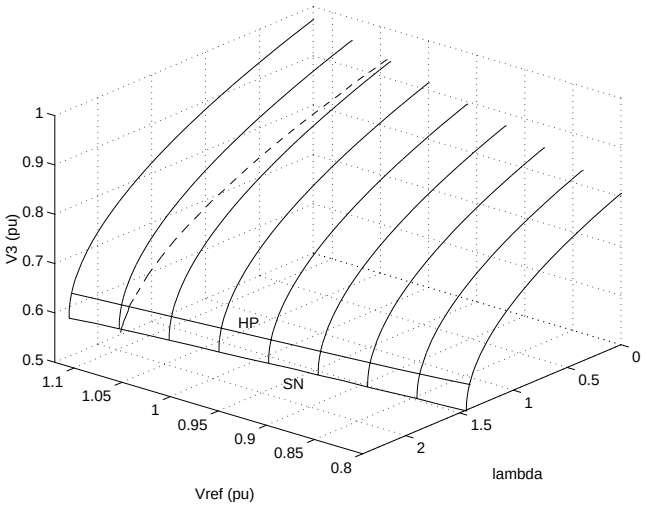

Fig. 2. Bifurcation diagram for the 3-bus test system without limits. The dashed line corresponds to the conventional power flow solutions.

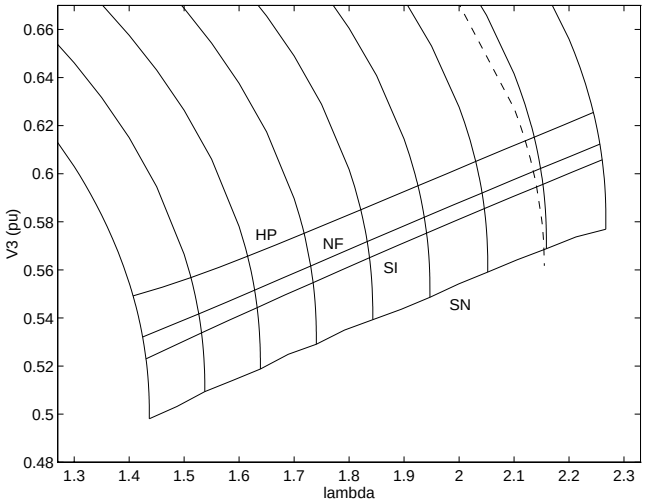

Fig. 3. Projection of the bifurcation diagram for the 3-bus test system without limits. The dashed line corresponds to the conventional power flow solutions.

point of maximum power transfer for this particular DAE system.

In both of these figures, a dashed line represents the solutions to the power flow problem as λ changes. It is important to indicate that the power flow equation used to obtain the results depicted here accurately represent the limits on the generator AVR [20]. This line, which basically corresponds to the PV curve, is obtained by assuming a fixed generator terminal voltage, allowing V_{ref} to change accordingly.

2) Case with limits: Hard limits of ±3.0 p.u. on the field voltage E_{fd} are added in this case to the AVR model. Figure 4 shows the behavior of E_{fd} versus V_{ref} and λ up to the SN bifurcation; no other bifurcations are depicted in this diagram to avoid cluttering up the picture. Figure 5 depicts V_3 versus the parameters V_{ref} and λ, plus some of the other bifurcations that occur "before" the SN. The generator does not reach a limit until the set-point V_{ref} attains a value of 1.0172 (point b on the curves). Hence, the bifurcation diagrams are basically the same as in the case with no limits, up to this V_{ref} value, with SNs occurring at points on the a-b section.

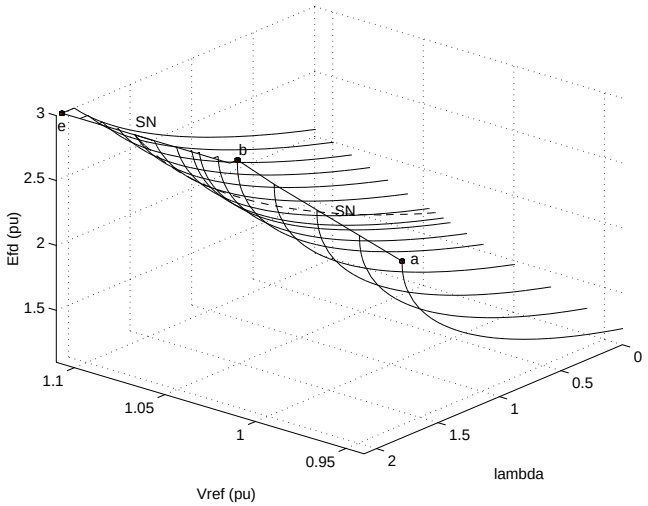

Fig. 4. Bifurcation diagram for the 3-bus test system with limits. The dashed line corresponds to the conventional power flow solutions.

The two dimensional diagram of Fig. 6 is used here to explain the effect of the different parameters and limits on the system bifurcations. On this figure, one can observe that, as λ changes for $1.0173<V_{ref}<1.0355$, the system first experiences an HP, then an NF and finally a SI bifurcation (SI1), as in the case without limits. However, when the generator reaches its E_{fd} limit, there is an immediate change in stability, with the system following a new stable bifurcation manifold (between the second SI bifurcation SI2 and point b). This turning point corresponds to an LI bifurcation .

For V_{ref} values between 1.0355 and 1.0392, the bifurcation diagram first reaches an HP and then an NF, followed by a LI bifurcation. At this point, one of the two positive real eigenvalues originated by the NF immediately moves to the left-hand side of the complex plane, while the remaining positive eigenvalue moves towards zero at the SN bifurcation. This phenomenon occurs until V_{ref} = 1.0393, when the NF manifold disappears.

For $1.0393<V_{ref}<1.0471$, the system initially experiences an HP and then an LI bifurcation (line c-d). The latter immediately undoes the unstable complex pair created by the HP, yielding two new real eigenvalues, one positive and another negative. The positive one eventually approaches zero at the SN bifurcation. The HP manifold disappears at V_{ref} = 1.0471; thus, for $V_{ref}>1.0471$ there is only an LI bifurcation, and a SN point. This LI bifurcation forces a negative eigenvalue to become immediately positive, and hence the system becomes immediately unstable when the generator reaches its limits.

Finally, for $V_{ref}>1.0590$, the system experiences a stable LI bifurcation, similar to a stable NF, before the SN bifurcation point. Observe that for $V_{ref}<1.0173$, there is an a-b line of SN bifurcation points; however, for $V_{ref} \geq 1.0173$ there is only one SN bifurcation point.

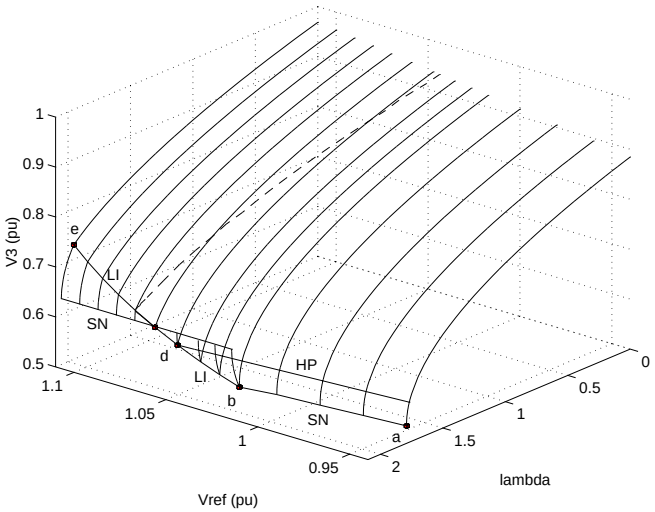

Fig. 5. Bifurcation diagram for the 3-bus test system with limits. The dashed line corresponds to the conventional power flow solutions.

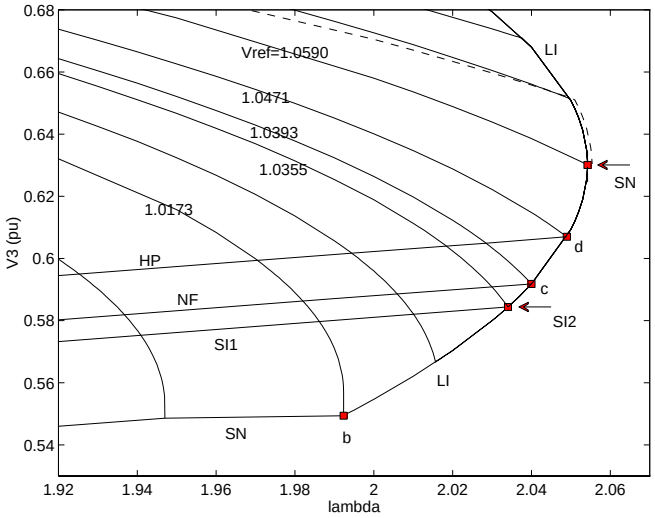

Fig. 6. Projection of the bifurcation diagram for the 3-bus test system. The dashed line corresponds to the conventional power flow solutions.

III. Practical Application

The previous section discussed the use of bifurcation theory to study the stability of the operating points of a small system, showing the influence of AVR droops and limits on the bifurcation diagrams. In this section, a similar approach is followed to study the bifurcation of the South-Brazilian system. This is a 213-bus system that comprises 20 aggregated generators, with the remaining of the Brazilian system being modeled as equivalent injections. A one-line sketch of this system is shown in Fig. 7.

The generator models used represent in detail saturation, PSS and AVR dynamics; the AVR models include hard (voltage field) and soft limits (current field, OEXL). The following first-order dynamic load model is used to represent some of the system loads [21]:

$$T_p \dot{x} = P_l V^a - x V^\alpha$$
$$T_q \dot{y} = Q_l V^b - y V^\beta \quad (7)$$

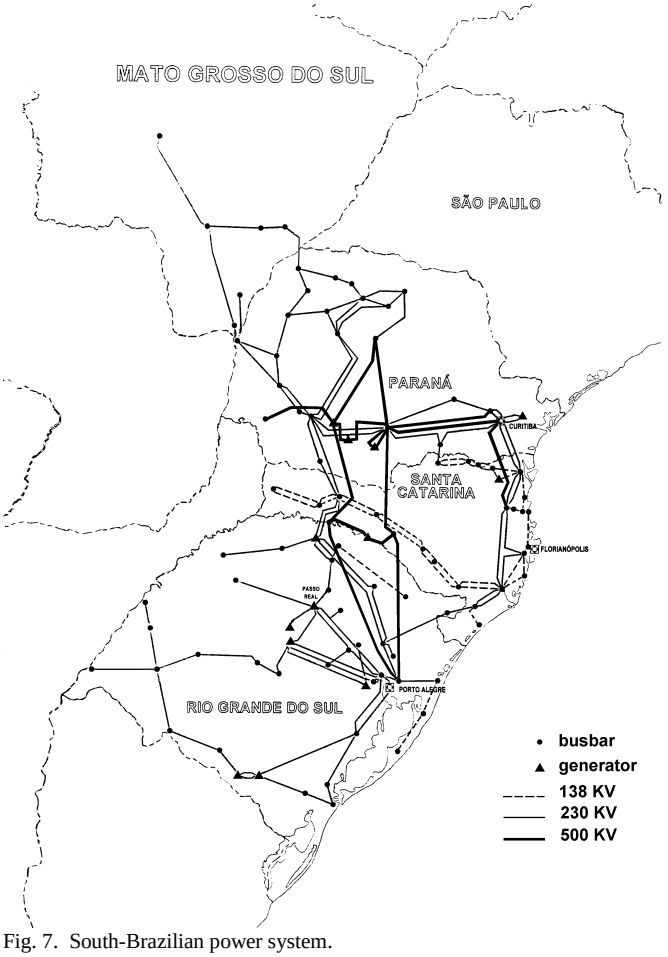

Fig. 7. South-Brazilian power system.

where T_p, T_q, a, α, b, and β are chosen constants, and P_l and Q_l are defined in (6); the x and y state variables are auxiliary variables used to model load power variations with respect to the bus voltage V in the time domain. All the dynamic models yield a system with 397 state variables and 426 algebraic variables, i.e. 823 DAEs and 397 eigenvalues to be analyzed at each operating point.

A. Bifurcation Analysis

The loads in this section are modeled in three different study cases using the dynamic model (7); a standard ZIP model is used in an additional test case to illustrate the effect of different load models in the bifurcation analysis of the system. Load model (6), which includes the bifurcation parameter λ, was used to represent load variations at buses 1182, 1225 and 1295, which correspond to hydraulic pumps for agricultural use that are known to have a significant influence in the stability of this system, especially as these increase. The reference voltage V_{ref} of the generator at bus 1162 was used to study the variation of a control parameter p, using a relatively wide range of values to study its effect on the system bifurcations. Although reference voltages in other generators were also considered, only variations on this particular generator are depicted here, as the results were very similar in all cases; presenting all of these results only complicates the illustration of the stability issues that are

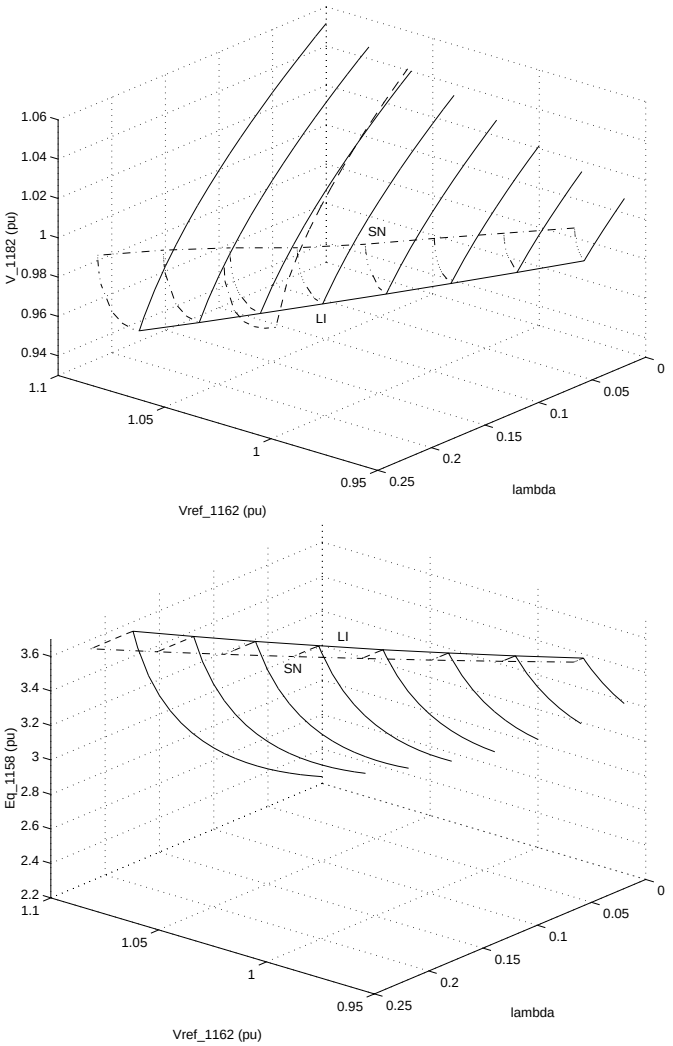

Fig. 8. Bifurcation diagrams for the South-Brazilian system (Case 1). The dashed line corresponds to the conventional power flow solutions; the dash-dot line represents the equilibria when limit recovery is not modeled.

discussed here, without giving any significant additional insight into the problem.

In all the figures presented here, a dashed line represents the solutions to the a power flow program as λ changes, considering that the power flow models used here accurately represent the limits on the generator AVRs, as discussed in [20].

Case 1. Assuming that T_p=25.0, a=0, α=0.4; and T_q=25.0, b=0, β=5.0 in load model (7), a constant power load model in steady state is represented, as a=b=0.0. The results obtained in this case are shown in Figs. 8 and 9, depicting the voltage at bus 1182 and the voltage E_q (proportional to the field current I_{fd}) in machine 1158 as functions of V_{ref} in machine 1162 and λ. The system experiences an unstable LI bifurcation due to the field current limits (OEXL) in generator 1158. For higher values of λ after this LI bifurcation point, the system will not present any equilibria when recovery from limits is modeled [1], i.e. this point will define the maximum loadability of the system. Limit recovery, however, was neglected in this case, so that the unstable equilibria branch

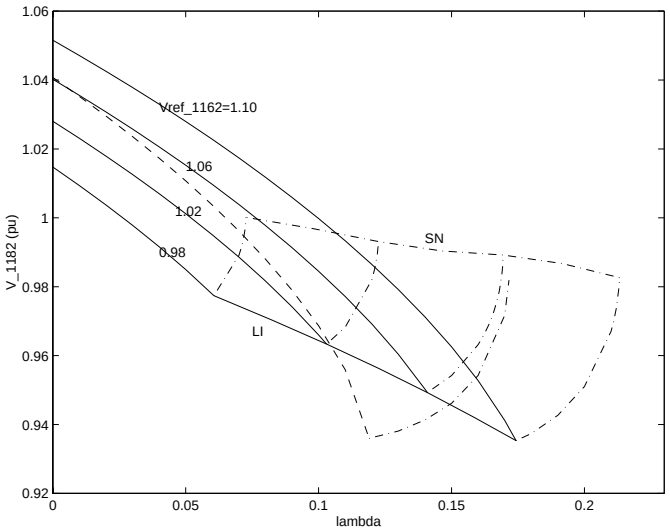

Fig. 9. Projection of the bifurcation diagram for the South-Brazilian system (Case 1). The dashed line corresponds to the conventional power flow solutions; the dash-dot line represents the equilibria when limit recovery is not modeled.

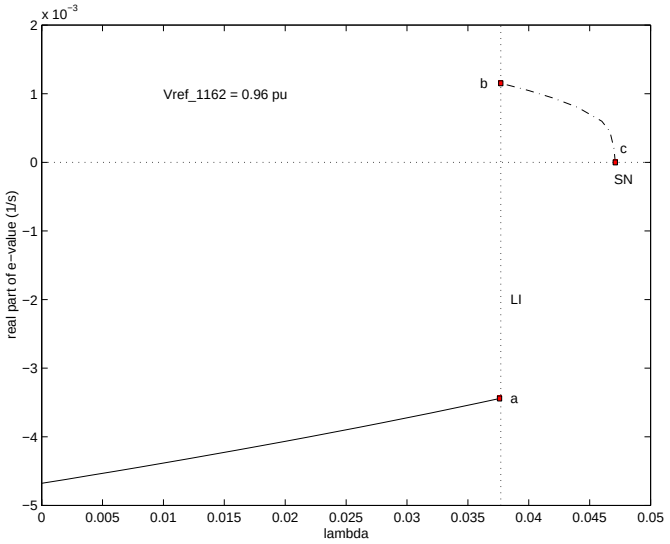

Fig. 10. Real part of the eigenvalue associated with the LI and SN bifurcations for the South-Brazilian system (Case 1). The dash-dot line represents the eigenvalues of equilibria when limit recovery is not modeled.

could be traced up to a SN point to allow for comparisons with other bifurcation diagrams presented in this paper.

The changes in the eigenvalue that lead the system to an unstable condition associated with an LI bifurcation are illustrated in Fig. 10, which depicts the real part of the eigenvalue versus changes in the loading parameter λ for $V_{ref\ 1162}$ = 0.96 p.u. Observe that when the system experiences the unstable LI bifurcation, one eigenvalue "jumps" from point 'a' to point 'b' on Fig. 10, becoming zero at point 'c', which forms part of the SN manifold depicted in Figs. 8 and 9. Similar eigenvalue plots can be obtained for all other cases discussed in this paper to illustrate the various bifurcations observed for the test system, but are not shown here due to space limitations.

Case 2. In this case, the load model parameters assumed are as follows: T_p=25.0, a=0.5, α=0.4; and T_q=25.0, b=0.5,

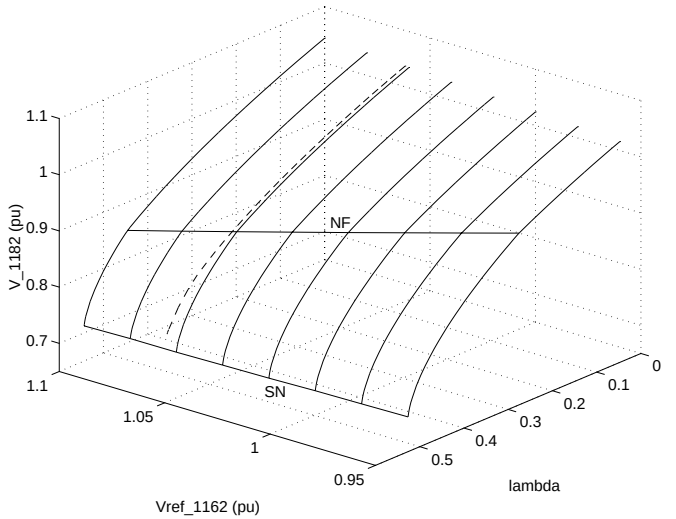

Fig. 11. Bifurcation diagram for the South-Brazilian system (Case 2). The dashed line corresponds to the conventional power flow solutions.

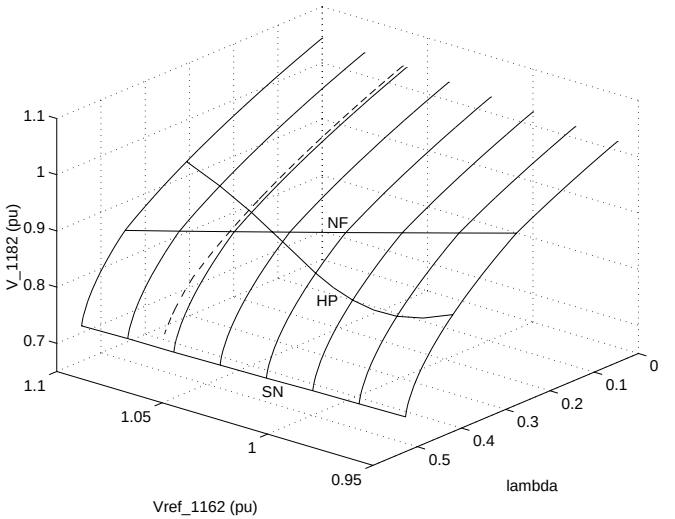

Fig. 13. Bifurcation diagram for the South-Brazilian system (Case 3). The dashed line corresponds to the conventional power flow solutions.

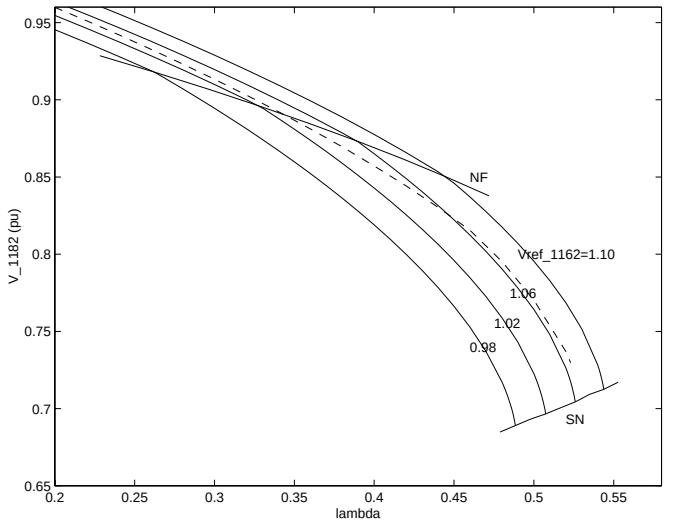

Fig. 12. Projection of the bifurcation diagram for the South-Brazilian system (Case 2). The dashed line corresponds to the conventional power flow solutions.

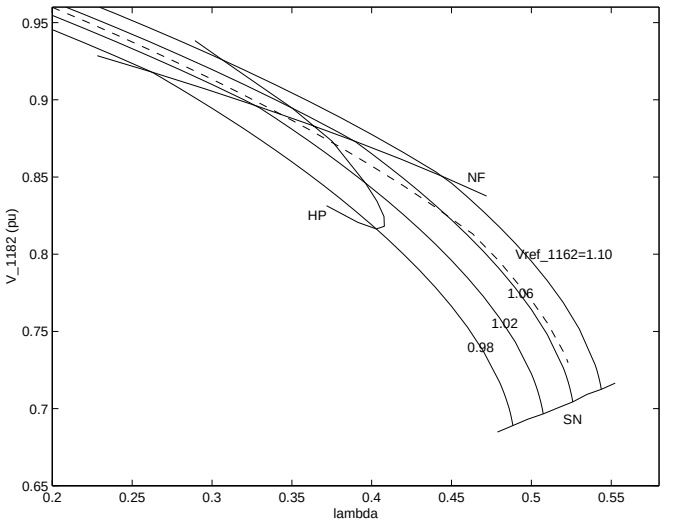

Fig. 14. Projection of the bifurcation diagram for the South-Brazilian system (Case 3). The dashed line corresponds to the conventional power flow solutions.

β=5.0. The parameters a and b have been changed with respect to the previous case, i.e. the loads are now voltage dependent in steady state, thus leading to different equilibrium points. The simulation results for this load model are shown in Figs. 11 and 12. Observe that he bifurcation diagram first reaches a stable NF, followed by a SN bifurcation; the NF bifurcation is associated with the OEXL in machine 1158.

Case 3. The load model parameters assumed in this case are as follows: T_p=25.0, a=0.5, α=0.4; and T_q=25.0, b=0.5, β=1.5. Observe that only the parameter β has changed with respect to Case 2, thus yielding the same equilibrium points. This results on the same NF and SN bifurcations; however, an HP bifurcation appears in this case, as illustrated in Figs. 13 and 14. There is a value for V_{ref}, at approximately 0.99, that yields the largest stability margin in this case. Observe in Figs. 13 and 14 that for some values of the V_{ref} parameter, an NF appears just before the HP, as suggested in [18]. However, this is not always the case, since, for other V_{ref} values, the NF is observed after the HP. These results complement the discussions on the possible physical meaning of NF bifurcations presented in [18].

Figure 15 illustrates the effect of the AVR droop on the stability analysis. The continuous line shows the equilibrium points obtained assuming a fixed V_{ref} value of generator 1162, whereas the dashed line corresponds to the conventional power flow model where the AVR set-point is assumed to change to maintain the generator terminal voltage constant. The difference between the slopes of the two curves up to the NF1 point, where the generator 1158 reaches its limits through an OEXL, is due to a load compensator connected at the input of AVR 1158; this device adjusts its output in order to cause a smooth raise on the terminal voltage when the reactive power generated increases, and is typically not modeled in a conventional power flow. When machine 1158 reaches its field current I_{fd} limits, the bus voltage drops faster due to the corresponding AVR droop. By including all device models in the power flow model, one obtains a maximum

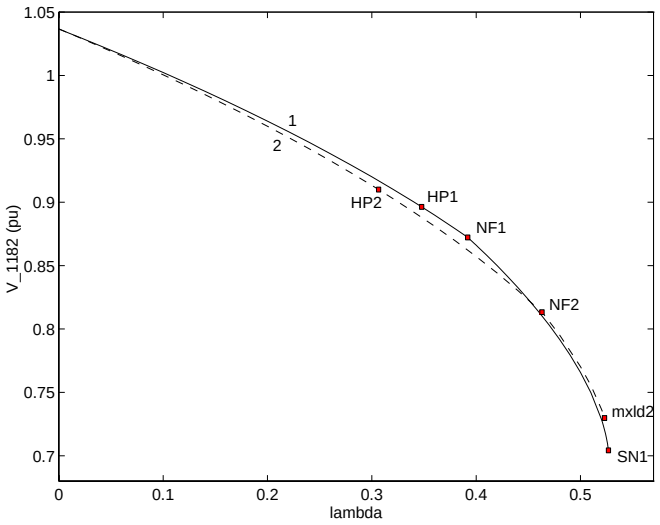

Fig. 15. Projection of the bifurcation diagram for the South-Brazilian system (Case 3). The dashed line corresponds to the conventional power flow solutions.

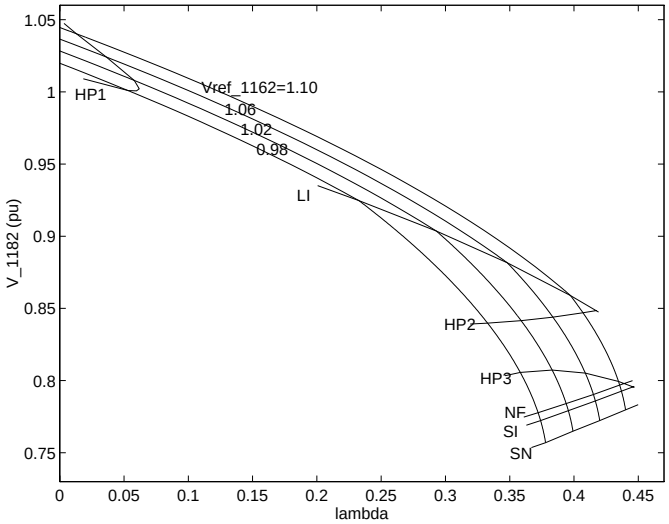

Fig. 16. Bifurcation diagram for the South-Brazilian system (Case 4).

loading point that corresponds to a SN bifurcation, whereas in the case of the conventional power flow model, the maximum loading (point 'mxld2' on Fig. 15) is not associated with to a SN bifurcation of the system. Observe also the significant differences in the "location" of the HP bifurcation for both models (points HP1 and HP2 on Fig. 15).

Case 4. In this case, the loads are modeled using a standard ZIP static model with 56% constant power and 44% constant current for both active and reactive powers. The results obtained in this case show the presence of an SI bifurcation, which was not observed in the previous three study cases for this system. This is due to the fact that the first-order dynamic load model (7) was used in the first 3 cases, basically removing the possibility of having the SI bifurcations associated with algebraic equations of load buses in the DAE model (2), since these equations are converted into differential equations by virtue of the dynamic load model used in these cases.

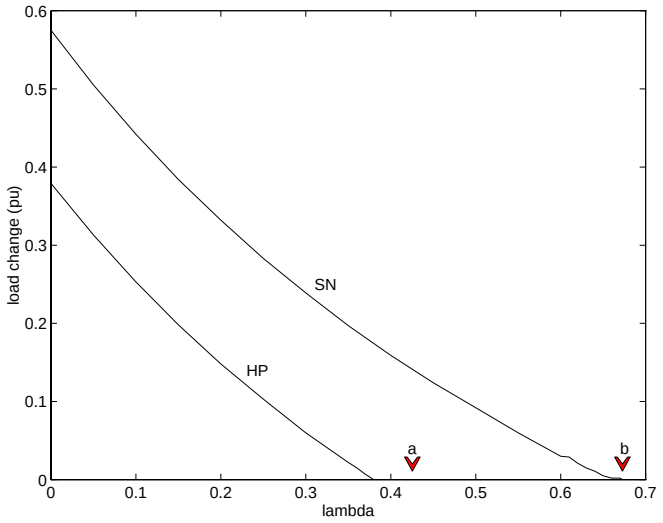

Fig. 17. Stability region for the South-Brazilian system.

The bifurcation diagram of Fig. 16 shows a rather rich dynamic behavior of the system as several types of bifurcations are encountered in this case. The first bifurcation, illustrated with the curve HP1, is a Hopf with 4.4 rad/s. This bifurcation is followed by a stable LI associated with the OEXL limitation of generator 1158. Then, another Hopf bifurcation (HP2) with high frequency (about 30 rad/s) is observed; the complex pair of eigenvalues associated with this Hopf is related to the NF and the SI bifurcations observed next as the load increases. Notice the close distance in terms of λ between the HP2 and the NF/SI bifurcations, which is due to the "high speed" of the associated eigenvalues. This pattern was observed in all simulations performed for this system when SI bifurcations are detected. The curve HP3 corresponds to another Hopf bifurcation with a frequency close to 7 rad/s.

B. Stability Regions

Figure 17 depicts the relative size of the stability region of the South-Brazilian system with respect to changes in the bifurcation parameter λ. These plots were obtained by determining, through time domain simulations, the largest instantaneous load change (plotted on the vertical axis in p.u.) that the system can withstand at the same load buses 1182, 1225, and 1295 without becoming unstable. This test gives a true sense of the size of the stability region without the need for any of the approximations required when using energy functions.

In this section, all loads were modeled using a ZIP static model assuming the following percentages of impedance (Z), current (I) and power (P) content on the active (P) an reactive (Q) powers:

a) For the SN case: P_Z=0, P_I=50%, P_P=50%; and Q_Z=100%, Q_I=0, Q_P=0.

b) For the HP case: P_Z=0, P_I=40%, P_P=60%; and Q_Z=100%, Q_I=0, Q_P=0.

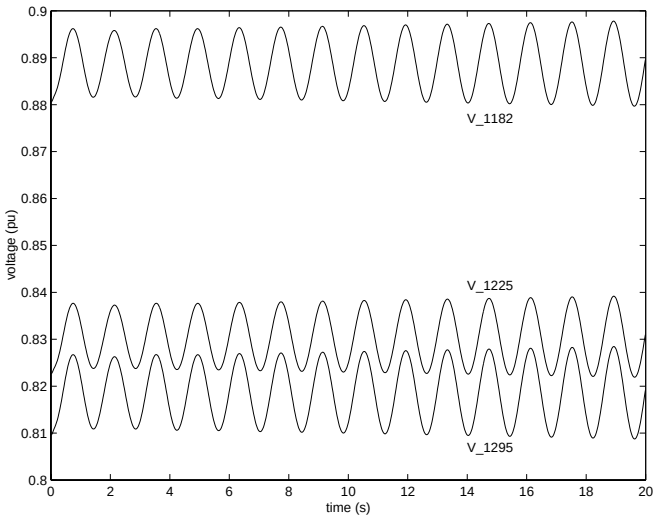

Fig. 18. Time domain response for the South-Brazilian system near point 'a' in Fig. 17 corresponding to a 0.7% load increase at buses 1182, 1225 and 1295.

These values were chosen so that the system loses stability due to either a SN or a HP as the loads of interest are increased. Dynamic models were not used in this case due to the limitations of the time domain simulation program used.

The actual HP and SN bifurcations occur at the points 'a' and 'b' on Fig. 17, respectively. In both cases the stability region decreases in a quasi linear manner as λ increases, reaching a "zero" value at the bifurcation point, or slightly before it in the case of the HP bifurcation, i.e. the "closer" to the bifurcation point, the "less stable" the system is; this is identical to what it has been observed using energy functions [11], [12]. Clearly, the stability region is affected by the location of the bifurcation point, as expected. In the HP case, the stability region seems to "disappear" slightly before the actual bifurcation point 'a', due to the fact that a 0.1% precision was used to simulate load changes.

Figure 18 depicts the results obtained from the time domain simulation for a sudden 0.7% load increase at buses 1182, 1225 and 1295, when the system is close to point 'a' in Fig. 17. Observe the oscillatory behavior of the bus voltages, which is to be expected given that the system undergoes a Hopf bifurcation associate with the sudden load increase.

It is interesting to mention that the results obtained here are agreeable with the operational experience of the actual system, where oscillatory as well as collapse problems have been observed in the past.

IV. Conclusions

The paper presents a thorough bifurcation analysis of detailed power system models, showing the effect of different control parameters and limits on the bifurcation and associated stability of the system. The issue of using conventional power flows versus the actual equilibrium equations to compute equilibrium points for bifurcation analysis is also discussed in detail.

This paper concentrates on showing the practical applications of bifurcation theory, as well as its stability implications for realistic power systems, demonstrating that these basic concepts can be readily and usefully applied to real systems. Applying the current and extensive bifurcation theoretical background to practical systems has not really been done before, as discussions have mainly concentrated on theoretical demonstrations using simple examples. The results presented here clearly show that the rather rich and complex dynamic behavior of actual systems can be thoroughly analyzed in practice using standard bifurcation tools.

References

[1] C. Cañizares, ed., "Voltage Stability Assessment, Procedures and Guides," IEEE/PES Power System Stability Subcommittee Special Publication, Final Draft, January 2001, http://www.power.uwaterloo.ca.

[2] A. A. P. Lerm, C. A. Cañizares, F. A. B. Lemos, and A. S. e Silva, "Multi-parameter Bifurcation Analysis of Power Systems," *Proceedings of the North American Power Symposium (NAPS)*, Cleveland, Ohio, pp. 76-82, Oct. 1998.

[3] R. Seydel, *Practical Bifurcation and Stability Analysis–From Equilibrium to Chaos*, Second Edition, Springer-Verlag, New York, 1994.

[4] C. A. Cañizares, "Conditions for saddle-node bifurcations in AC/DC power Systems," *Int. J. of Electric Power & Energy Systems*, Vol. 17, No. 1, pp. 61-68, Feb. 1995.

[5] B. C. Lesieutre, P. W. Sauer, and M. A. Pai, "Why Power/Voltage Curves Are Not Necessarily Bifurcation Diagrams," *25th North American Power Symposium*, Washington, pp. 30-37, Oct. 1993.

[6] M. A. Pai, P. W. Sauer, and B. C. Lesieutre, "Static and Dynamic Nonlinear Loads and Structural Stability in Power Systems," *Proceedings of the IEEE*, Vol. 83, pp. 1562-1572, Nov. 1995.

[7] V. Venkatasubramanian, H. Schättler, and J. Zaborszky, "Dynamics of Large Constrained Nonlinear Systems–A Taxonomy," *Proceedings of the IEEE*, Vol. 83, pp. 1530-1561, Nov. 1995.

[8] I. Dobson and L. Lu, "Immediate Change in Stability and Voltage Collapse When Generator Reactive Power Limits are Encountered," *Proceedings of Bulk–Power Voltage Phenomena II – Voltage Stability and Security*, Maryland, pp. 65-73, Aug. 1991.

[9] C. A. Cañizares and F. L. Alvarado, "Point of Collapse and Continuation Methods for Large AC/DC Systems," *IEEE Transactions on Power Systems*, Vol. 8, No. 1, pp. 1-8, Feb. 1993.

[10] B. Lee and V. Ajjarapu, "A Piecewise Global Small-disturbance Voltage-stability Analysis of Structure-preserving Power System Models", *IEEE Transactions on Power Systems*, Vol. 10, No. 4, pp. 1963-1971, Nov. 1995.

[11] T. J. Overbye and C. L. DeMarco, "Voltage Security Enhancement Using Energy Based Sensitivities," *IEEE Transactions on Power Systems*, Vol. 6, No. 3, pp. 1196-1202, Aug. 1991.

[12] C. A. Cañizares, "Calculating Optimal System Parameters to Maximize the Distance to Saddle-node Bifurcations," *IEEE Trans. Circuits and Systems–I*, Vol. 45, No. 3, pp. 225-237, March 1998.

[13] D. J. Hill and I. M. Y. Mareels, "Stability Theory for Differential/Algebraic Systems with Application to Power Systems," *IEEE Trans. Circuits and Systems*, Vol. 37, No. 11, pp. 1416-1423, Nov. 1990.

[14] V. Venkatasubramanian, H. Schattler, and J. Zaborszky, "A Taxonomy of the Dynamics of the Large Power Systems with Emphasis on its Voltage Stability," *Proc. Bulk Power System Voltage Phenomena II–Voltage Stability and Security*, ECC Inc., pp. 9-52, Aug. 1991.

[15] I. Dobson, "The irrelevance of load dynamics for the loading margin to voltage collapse and its sensitivities," *Proc. Bulk Power System Voltage Phenomena III–Voltage Stability and Security*, ECC Inc., pp. 509-518, Aug. 1994.

[16] J. Guckenheimer and P. Holmes, *Nonlinear Oscillations, Dynamical Systems and Bifurcation of Vector Fields*. Applied Mathematical Sciences, Springer-Verlag, New York, 1986.

[17] H. G. Kwatny, R. F. Fischl, and C. O. Nwankpa, "Local Bifurcation in Power Systems: Theory, Computation, and Application," *Proceedings of the IEEE*, Vol. 83, pp. 1456-1483, Nov. 1995.

[18] I. Dobson, J. Zhang., S. Green, H. Engdahl, and P. Sauer, "Is Strong Modal Resonance a Precursor to Power System Oscillations?," *IEEE Trans. Circuits and Systems-I*, Vol. 48, Bo. 3, pp. 340-349, March 2001.

[19] C. A. Cañizares and S. Hranilovic, "Transcritical and Hopf Bifurcations in AC/DC Systems," *Proc. Bulk Power System Voltage Phenomena III– Voltage Stability and Security*, ECC Inc., pp. 105-114, Aug. 1994.

[20] A. A. P. Lerm, F. A. B. Lemos, A. S. e Silva, and M. Irving, "Voltage Stability Assessment with Inclusion of Hard Limits," *IEE Proceedings - Part C, Generation, Transmission and Distribution*, Vol. 145, No. 5, pp. 505-510, Sept. 1998.

[21] W. Xu and Y. Mansour, "Voltage Stability Using Generic Dynamic Load Models," *IEEE/PES Winter Meeting*, Columbus, OH, Jan. 1993.

André Arthur Perleberg Lerm received his degree in Electrical Engineering from Universidade Católica de Pelotas, Brazil in 1986, and the M.Sc. and Ph.D. degrees in Electrical Engineering, both from Universidade Federal de Santa Catarina, Brazil, in 1995 and in 2000, respectively. As a part of his Ph.D. program he joined the University of Waterloo, Canada, for a split Ph.D. in 1997. Since 1987 and 1988, he has been with Universidade Católica de Pelotas and Centro Federal de Educação Tecnológica - RS, respectively. His main research interests are in the area of power systems dynamics, voltage stability and systems modeling.

Claudio A. Cañizares received the Electrical Engineer diploma (1984) from the Escuela Politécnica Nacional (EPN), Quito-Ecuador, where he held different positions from 1983 to 1993. His M.Sc. (1988) and Ph.D. (1991) degrees in Electrical Engineering are from the University of Wisconsin-Madison. Dr. Cañizares is currently an Associate Professor at the University of Waterloo and his research activities are mostly concentrated on the study of computational, modeling, and stability issues in ac/dc/FACTS power systems.

Aguinaldo Silveira e Silva received his degree in Electrical Engineering from the Universidade Federal de Parana, Brazil in 1977, and the M.Sc. and Ph.D. degrees in Electrical Engineering from Universidade Federal de Santa Catarina, Brazil, in 1982 and UMIST, UK, in 1990, respectively. Since 1980, he has been with the Universidade Federal de Santa Catarina. His main research interests are in the area of power systems dynamics and control applications.